Optical vortices in six-wave mixing

Matt M. Coles, Mathew D. Williams, and David L. Andrews*
School of Chemistry, University of East Anglia, Norwich NR4 7TJ, United Kingdom

ABSTRACT

Optical vortex light engendered with integer units of orbital angular momentum (OAM) may be involved in frequency upconversion. Second harmonic generation is usually forbidden in isotropic media due to parity constraints, but it becomes allowed by six-wave mixing. Here, we present a rigorous quantum analysis for the case of a Laguerre-Gaussian input beam comprising photons endowed with a single unit of OAM. Such a process gives rise to the novel entanglement of orbital momentum in two emergent photons; it transpires that the mechanism delivers a harmonic output whose polarization is essentially parallel to the incident radiation. This investigation ascertains the character of the emission, both under forward propagation and back-reflection geometries, and identifies in detail the form of distribution in the entangled total orbital momentum. A distinctive conical spread, originating from the entangled distribution in the emission pair, affords a potential means to determine the individual angular momenta.

Keywords: multiphoton process, optical vortex, second harmonic generation, Laguerre-Gaussian beam, six-wave mixing, structured light, nonlinear optics.

1. INTRODUCTION

When an optically nonlinear medium is irradiated with intense laser light that has a structured wavefront, the transmitted beam can display a variety of features associated with the modal complexity of the input. For example, in second harmonic generation (SHG), the input of optical vortex light will produce output in which each frequency-doubled photon also carries twice the orbital angular momentum of the absorbed photons.[1-2] In common with all even harmonics, SHG is supported by an optical susceptibility tensor of odd order, and it therefore generally occurs in a non-centrosymmetric material. In fact, the process is forbidden in isotropic media to all multipole orders.[3]

However, the possible occurrence of SHG in a centrosymmetric medium is rigorously precluded only at relatively low levels of intensity – where the prospects for higher order interactions are remote. At sufficiently high intensities one can envisage a situation in which two second harmonic processes occur simultaneously, within the limits of quantum uncertainty, thereby involving an even number of photons and thus supported by an optical susceptibility tensor of odd order. To be precise, SHG is then allowed by a six-wave process in which four photons of pump input are converted into two photons of harmonic output, the latter emerging equally disposed on the surface of a cone (due to the constraints of wave-vector matching and optical dispersion). An experimental confirmation of exactly this type of higher order nonlinear optical phenomenon has been demonstrated by Boyd *et al.*,[4] showing a third-harmonic signal emerging from sapphire in a tightly confined cone of forward emission. This follows the earlier predictive work of Andrews *et al.*, developing theory that was followed by the first experimental reports on six-wave mixing (SWM).[5-10]

Here we show that six-wave mixing with an input conveying orbital angular momentum (OAM) shows new optical effects. Beams of light that have the capacity to convey OAM are associated with a helically formed wavefront; often called 'twisted beams', Laguerre-Gaussian (LG) modes are the most familiar type. Such modes are generally characterized by a topological charge l, signifying the number of wavelengths over which each of l intertwined components of the wavefront complete one cycle about the beam axis. Accordingly, it emerges that each photon in the beam conveys an OAM of $l\hbar$, independently of any spin angular momentum associated with circular polarization. Deployed in the pursuit of six-wave mixing, in which each harmonic conversion event produces two photons, it proves possible for both linear momentum and OAM conservation laws to be satisfied in more than one possible outcome. As we shall show, the process displays novel characteristics of interest for the on-going development of quantum state entanglement with heralded photon generation.

Complex Light and Optical Forces VIII, edited by David L. Andrews, Enrique J. Galvez, Jesper Glückstad,
Proc. of SPIE Vol. 8999, 89990Y · © 2014 SPIE · CCC code: 0277-786X/14/$18 · doi: 10.1117/12.2036767

2. THE PURSUIT OF ENTANGLED OAM

2.1 The rationale for six-wave mixing

Our aim is to produce, in each interaction, the release of two state-entangled photons, of the same wavelength but propagating in different directions, and with a distribution of potentially different quanta of OAM. There is a strong logic leading to the conclusion that SWM affords the most promising avenue to explore, in the sense that it involves the lowest order of optical nonlinearity that can deliver the sought characteristics. For example, in attempting to achieve this aim based on interactions involving a single photon input, which in this case would signify the process of down-conversion, the open medium result would be a spectrum of sum-frequency outputs, rather than the sought degenerate down-conversion that would be necessary to release two photons of the same wavelength. The way to secure the latter outcome is usually to deploy a cavity configuration (or a secondary input) selecting one output mode for stimulated emission, but that would effectively determine the OAM of that beam according to the input; no distribution of outcomes could then ensue. Similar arguments apply to degenerate four-wave mixing, in which the problems would be compounded by having all photons of identical frequency. Processes involving three input and two output photons, *i.e.* five-wave mixing, present extraordinarily challenging experimental difficulties, even without the involvement of OAM: although the theory was worked out many years ago, there are remarkably few reports of such processes. It is therefore six-wave mixing, for which there have been numerous theoretical and experimental measurements, that presents the best opportunities.

2.2 Quantum electrodynamical development

To develop the theory, we therefore begin by deriving the probability amplitude for SWM.[11] Using well established methods the intensity distribution may then be calculated using the Fermi rule. The quantum amplitude is accordingly derived from sixth order perturbation theory,[6] using the form:

$$M_{FI}^{(6)} = \sum_{R,S,T,U,V \neq I,F} \frac{\langle F | H_{\text{int}} | V \rangle \langle V | H_{\text{int}} | U \rangle \langle U | H_{\text{int}} | T \rangle \langle T | H_{\text{int}} | S \rangle \langle S | H_{\text{int}} | R \rangle \langle R | H_{\text{int}} | I \rangle}{(E_I - E_R)(E_I - E_S)(E_I - E_T)(E_I - E_U)(E_I - E_V)}, \tag{1}$$

where I and F denote initial and final system states, R, S, T, U, V, denote virtual intermediate states, and E is the energy of a state designated by the subscript. In the electric dipole approximation the interaction Hamiltonian is given by $H_{\text{int}} = -\varepsilon_0^{-1} \boldsymbol{\mu} \cdot \mathbf{d}^{\perp}$ where $\boldsymbol{\mu}$ is the electric dipole vector and $\mathbf{d}^{\perp}$ is the transverse electric displacement field which, in a quantum optical representation is developed in the form of a mode expansion using photon creation and annihilation operators. To address vortex radiation, without loss of generality, we specifically use a mode expansion cast in terms of Laguerre-Gaussian modes (a linear combination of which can describe any electromagnetic field):

$$\mathbf{d}^{\perp}(\mathbf{r}) = i \sum_{\mathbf{k},\eta,l,p} \left(\frac{\hbar c k \varepsilon_0}{2\Omega} \right)^{\frac{1}{2}} \left\{ \mathbf{e}_{l,p}{}^{(\eta)}(\mathbf{k}) a^{(\eta)}(\mathbf{k}) f_{l,p}(r) e^{ikz - il\varphi} - \overline{\mathbf{e}}_{l,p}{}^{(\eta)}(\mathbf{k}) a^{\dagger(\eta)}(\mathbf{k}) f_{l,p}(r) e^{-ikz + il\varphi} \right\}. \tag{2}$$

Here, $f_{l,p}(r)$ represents the radial distribution function of the LG mode with radial number p, azimuthal index l, and the right hand term is the Hermitian conjugate of the left.

In applying this expansion to identify the form of result from equation (1), it is necessary to sum over all time orderings for the six individual photon interactions, in each case identifying the populations of each optical mode in the system states R, S, T, U, V. It is readily determined that there are fifteen quantum pathways linking the initial radiation state (with four input photons) to the final state (two emitted photons), each of them corresponds to one of the Feynman graphs, and hence a contributory quantum amplitude, for the six-wave process. Interpreting the Feynman diagrams delivers the form of the material states, thus providing the structure for the associated optical susceptibility tensor – in this case a fifth rank tensor $\boldsymbol{\chi}^{(5)}$. The full result for the quantum amplitude for six-wave conversion at a position $\mathbf{r}$ now emerges in a form that is readily cast in terms of the Cartesian components of polarization vectors for the input and output, $\mathbf{e}$ and $\mathbf{e}'$ respectively. Using the usual implied summation over repeated tensor indices, we have:

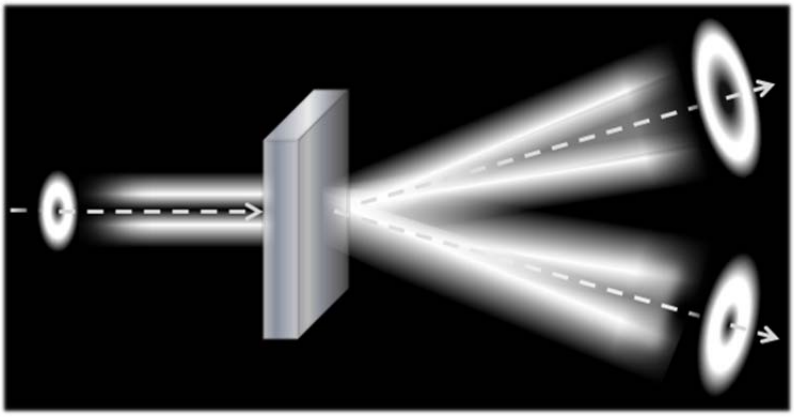

Figure 1. Passage of an $l = 1$ LG mode through a centrosymmetric medium, resulting in second harmonic generation.

$$M_{FI}(\mathbf{r}) = \sqrt{3}\left(\frac{\hbar ck}{\sqrt{2}\varepsilon_0\Omega}\right)^3 \bar{e}_i''\bar{e}_j' e_k e_l e_m e_n \chi^{(5)}_{(ij)(klmn)} e^{i(4\mathbf{k}-\mathbf{k}'-\mathbf{k}'').\mathbf{r}}. \tag{3}$$

In the six-wave process of interest, for which the beam geometry is depicted in Fig. 1, four photons of wave-vector **k**, polarization η and circular frequency ω, are converted to two photons, the latter having wave-vectors **k′**, **k″** and polarizations η', η'', respectively. By virtue of energy conservation, both of the output photons have the same frequency $\omega' = 2\omega$; however, allowing for the effects of optical dispersion they are allowed to have different directions of propagation.

The result (3) for the SWM quantum amplitude assumes a basis of Fock (number) states for the input radiation, quantized in a volume Ω. The quantization volume is here defined as the volume that contains the energy of the four input and two output photons. Also in Eq. (3), $\chi^{(5)}_{(ij)(klmn)}$ signifies a component of the index-symmetrized nonlinear susceptibility tensor, whose structure can be depicted and evaluated by using a previously reported method.

$$\chi^{(5)}_{(ij)(klmn)} = -\frac{1}{48}\sum_{\substack{r,s,t,u,v \\ \mathbf{k},\eta,l,p}}\left[\left\{\frac{\mu_i^{0v}\mu_j^{vu}\mu_k^{ut}\mu_l^{ts}\mu_m^{sr}\mu_n^{r0}}{[E_{r0}-\hbar ck][E_{s0}-2\hbar ck][E_{t0}-3\hbar ck][E_{u0}-4\hbar ck][E_{v0}-2\hbar ck]}+\ldots\right\}\right.$$
$$\left.+\{perm(i,j)\,perm(k,l,m,n)\}\right], \tag{4}$$

where *perm* denotes all permutations of the index set in parentheses. It transpires that the term explicitly given in Eq. (4), the first of fifteen that feature within curly braces, delivers the major contribution. This term dominates over the other contributions because each of its denominator factors can, in effecting the corresponding summations over electronic states *r*, *s*, *t*, *u*, *v*, produce a diminutive result.

Before proceeding further, it can be observed that the SWM phenomenon of interest is also supported by a very different beam geometry, as shown in Fig. 2. Here, an LG beam transmitted through a dispersive medium impinges at normal incidence upon an interface with a less dense medium, coated with an ultra-thin layer of vacuum deposited silver, at which internal reflection occurs. In this case, the connection between the linear momenta of the input and output beams has to be interpreted differently: the cases of forward propagation and back-reflection are summarized in the following:

$$\mathbf{k}' + \mathbf{k}'' = \pm 4\mathbf{k}\ , \tag{5}$$

where the positive sign corresponds to the former, and the negative sign the latter, case. In both cases a conical form can be anticipated for the emergent harmonic in dispersive media, its apical angle determined by the refractive index of both the input and emergent radiation.

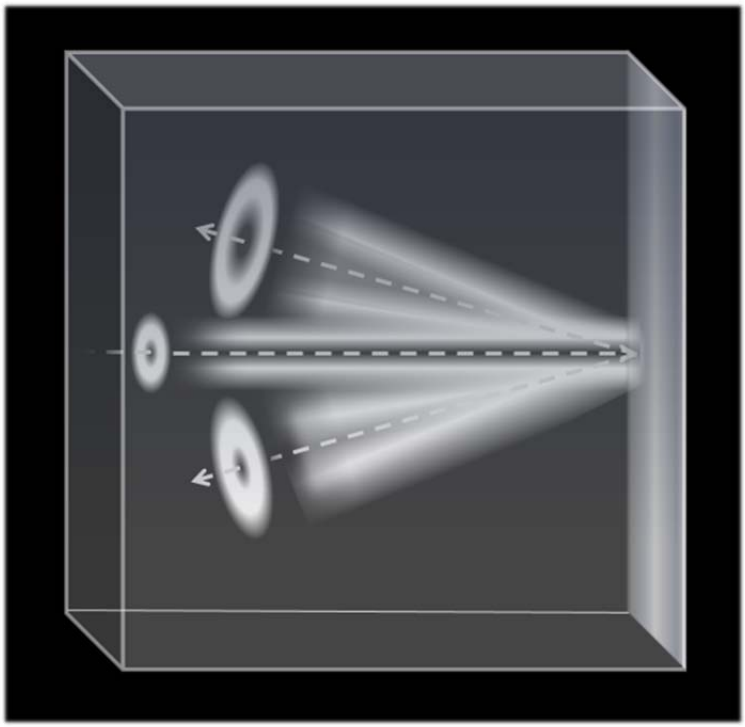

Figure 2. Reflection geometry for SWM with LG input radiation.

To continue, it is now expedient to model a random distribution of optical center orientations in the conversion material, as for example would relate to the experimental measurements of SWM that have been performed with fused silica glass.[4] As a parametric process, the amplitudes for different optical centers add constructively.[12] The ensuing rate emerges as:

$$\Gamma \sim \left| \left(\bar{\mathbf{e}}' \cdot \bar{\mathbf{e}}''\right)\left(\mathbf{e}\cdot\mathbf{e}\right)^2 \left\{ 23\chi^{(5)}_{(\lambda\lambda)(\mu\mu\nu\nu)} - 20\chi^{(5)}_{(\lambda\mu)(\lambda\mu\nu\nu)} \right\} + \left(\bar{\mathbf{e}}' \cdot \mathbf{e}\right)\left(\bar{\mathbf{e}}'' \cdot \mathbf{e}\right)\left(\mathbf{e}\cdot\mathbf{e}\right) \left\{ -20\chi^{(5)}_{(\lambda\lambda)(\mu\mu\nu\nu)} + 32\chi^{(5)}_{(\lambda\mu)(\lambda\mu\nu\nu)} \right\} \right|^2, \tag{6}$$

where Greek letter indices denote laboratory frame coordinates. As both terms are dependent on $\left(\mathbf{e}\cdot\mathbf{e}\right)$, the use of a circularly polarized basis would deliver a vanishing result; the most efficient conversion rate is obtained by the use of plane polarized input radiation. Resolving the output into plane polarized components gives:

$$\Gamma \sim \left| \left\{ 3\chi^{(5)}_{(\lambda\lambda)(\mu\mu\nu\nu)} + 12\chi^{(5)}_{(\lambda\mu)(\lambda\mu\nu\nu)} \right\} \right|^2, \tag{7}$$

for polarizations parallel to the input, $\left(\bar{\mathbf{e}}' \cdot \mathbf{e}\right) = \left(\bar{\mathbf{e}}'' \cdot \mathbf{e}\right) = \left(\mathbf{e}\cdot\mathbf{e}\right) = \left(\bar{\mathbf{e}}' \cdot \bar{\mathbf{e}}''\right) = 1$, and

$$\Gamma \sim \left| \left\{ 23\chi^{(5)}_{(\lambda\lambda)(\mu\mu\nu\nu)} - 20\chi^{(5)}_{(\lambda\mu)(\lambda\mu\nu\nu)} \right\} \right|^2, \tag{8}$$

for polarizations perpendicular to the input, $\left(\bar{\mathbf{e}}' \cdot \mathbf{e}\right) = \left(\bar{\mathbf{e}}'' \cdot \mathbf{e}\right) = 0$; $\left(\mathbf{e}\cdot\mathbf{e}\right) = \left(\bar{\mathbf{e}}' \cdot \bar{\mathbf{e}}''\right) = 1$. For materials in which all tensor components have a similar value and sign, such that $\chi^{(5)}_{(\lambda\lambda)(\mu\mu\nu\nu)} = \chi^{(5)}_{(\lambda\mu)(\lambda\mu\nu\nu)}$, the above results suggest the emergent radiation will be primarily polarized parallel to the input.

3. QUANTUM ENTANGLEMENT OF EMITTED HARMONIC PHOTONS

In our computer simulations, output fields are determined at a distance of several hundred output wavelengths from the location of optical conversion, with parameters chosen to simulate a pump laser at wavelength 800 nm, with l = 1 radial profile, at focus in the nonlinear conversion material. To estimate the cone angle, determined by the inverse cosine of the refractive index ratio for the output, relative to the input, wavelength, we use the results for third harmonic generation of Boyd *et al.*,[4] corresponding to approximately 10°-12° - signifying consistency with the paraxial approximation to within 1%. Furthermore, the beam-waist is set at 299.4 microns, which imposes a Rayleigh range of 444 μm. We have computed the various contributions to the output with different orbital angular momenta by use of the rate equation with identical initial and differing final states, assuming the beam-waist remains unchanged.

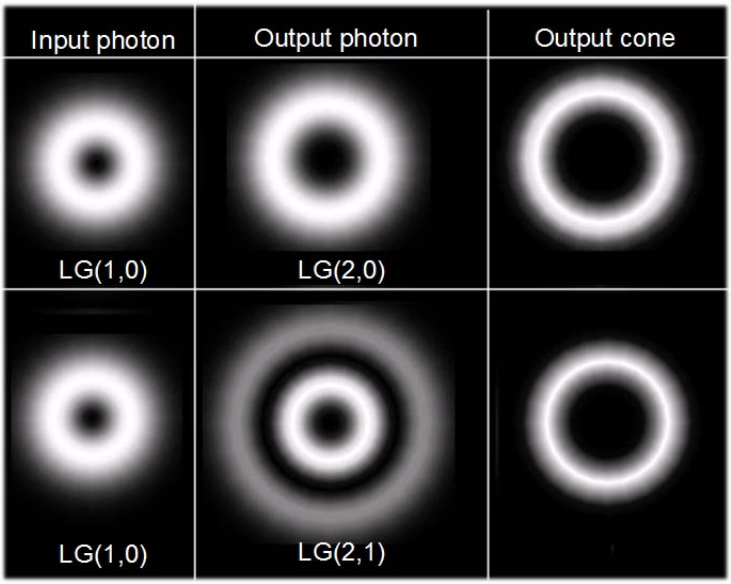

Figure 3. Intensity distributions of the SWM input and output, with varying radial index, p. The column headed 'Output photon' shows the intensity distributions centered upon the propagation direction. The wave-vector of the LG(2, 0) cone is clearly much sharper than for the LG(2,1) cone output, owing to the wider radial profile of the LG(2,1) photon mode. The 'Output cone' column shows the distribution of output propagation directions, each point on which represents the center of a modal distribution.

Fig. 3 shows plots of the "output cone" intensity, corresponding to the results of the rate equation, Eq. (6). Here we consider the process involving four l_0 = 1 input photons. With $l_1 \geq l_2$, there are three possible pairs of emergent photons: (l_1, l_2) = (2,2); (3,1); (4,0). Interestingly, while the output profile displays no structural differences between the unique combinations of emergent pairs, for p = 0, the relative magnitudes have a simple relationship. Precisely, the intensity of the (3,1) signal is 4 times the (4,0), whereas the (2,2) signal is bigger by a factor of 6. This binomial series expansion form arises without any assumption of combinatorial weighting, and independently verifies the calculations. Furthermore, the pairing of (l_1, l_2) values clearly indicates quantum entanglement between the generated optical states, as has recently been observed in other studies with optical vortex beams.[13-15] For output LG modes with p > 0, the beam width, w, increases outwards with a monotonic dependence on p, from the p = 0 counterpart. Hence the Fermi rate, which inherits a w^{-2p} dependence from the radial distribution functions, delivers successively smaller contributions for non-zero p modes. Even so, the slight variation in the conical emission for modes with p > 0 is investigated in the lower row of Fig. 3.

Using a representation in which modal states are differentiated only by orbital angular momentum (accommodating photons propagating outwards in any direction along the emission cone) the ω' emission is thus cast in a form that comprises a superposition of product states expressible as $|l\rangle_{\mathbf{k}'}|4-l\rangle_{\mathbf{k}''}$, with a corresponding intensity distribution given by the binomial coefficients ${}_4C_l$. Each of these product states carries entangled information on the orbital angular momentum conveyed by photons emitted on opposing sides of the cone. For example a measurement of l = 4 in one direction signifies a counterpart photon with l = 0 in the other. Since the labelling is arbitrary, $|l_1\rangle_{\mathbf{k}'}|l_2\rangle_{\mathbf{k}''}$ is indistinguishable from $|l_2\rangle_{\mathbf{k}'}|l_1\rangle_{\mathbf{k}''}$ and we can choose $l_1 \geq l_2$ and write the product state simply as $|l_1 : 4-l_1\rangle$ Then it emerges that the emitted field has an overall form given by a normalized state vector taking the form:

$$\frac{1}{2\sqrt{2}}\left\{|4:0\rangle + 2|3:1\rangle + \sqrt{3}|2:2\rangle\right\} \quad . \tag{9}$$

Thus, prior to measurement, the emitted electromagnetic field exists in a superposition state with different allowed (l_1, l_2) combinations. The detection of one photon with a specific OAM l_1 in the sorted output can be considered to herald its partnering photon with the complementary OAM value $l_2 = 4l_0 - l_1$, a situation similar to the Einstein-Podolsky-Rosen 'paradox'. In this respect, the SWM interaction displays some similarities with optically parametric down-conversion, which is more familiarly associated with the production of entangled light.[16] However, although both generate two photons of output, the Pascal's triangle combinatorial weighting, revealed in the SWM output distribution here, stands it in stark contrast to down-conversion. There are also striking differences between the characteristics of the SWM process and recent observations of unexpectedly weighted topological charge distributions in four-wave coupling interactions.[17]

The result of Eq. (9) signifies a new departure in the field of OAM: to our knowledge this is the first time that a superposition of modes, propagating in discernibly different directions with widely differing units of angular momentum, has been formulated. As such, it represents one example of a range of possibilities for future developments.

4. CONCLUSION

Recently, there has been rapidly growing interest in the interaction of singular light with nonlinear optical materials,[18] notably with four-wave parametric processes.[19-20] The process described in this paper is a higher-order interaction that reveals further characteristics deeply connected with both the quantum and nonlinear optical character of the set-up. For simplicity, and also to directly connect with the realm of most practicable experimental measurements, we have considered the measurable form of the output in a region well removed from the conversion material – a distance of around one hundred input or two hundred output wavelengths. Clearly, in a closer region there will be significant overlap of the ring structures across the emission cone, and closer still there will be near-field features further complicating the structure of the emergent fields. However, in such regions where there is greater uncertainty over the resolvable angle of emission, it can be anticipated that there will be manifestations of an increasing angle-angular momentum quantum uncertainty.[21-24] In the long-range, the angular distribution of the output presents a useful way to experimentally divert beam components, even individual photons, towards devices that can resolve their orbital angular momentum content, for example using one of the recently reported sorting and detection mechanisms.[25-27,15,28] As we have shown, systems exploring the distribution of orbital angular momentum in the twin harmonic outputs – in both propagating and reflection geometries – present new avenues to explore entanglement features in the production and interrogation of structured light.[15]

ACKNOWLEDGEMENTS

The authors would like to thank EPSRC and University of East Anglia for funding this research.

REFERENCES

[1] Dholakia, K., Simpson, N. B., Padgett, M. J. and Allen, L., "Second-harmonic generation and the orbital angular momentum of light," Phys. Rev. A 54, 3742-3745 (1996).

[2] Dávila Romero, L. C., Andrews, D. L. and Babiker, M., "A quantum electrodynamics framework for the nonlinear optics of twisted beams," J. Opt. B: Quantum Semiclass. Opt. 4, 66 (2002).

[3] Andrews, D. L., "Harmonic generation in free molecules," J. Phys. B: At. Mol. Opt. Phys. 13, 4091-4099 (1980).

[4] Moll, K. D., Homoelle, D., Gaeta, A. L. and Boyd, R. W., "Conical Harmonic Generation in Isotropic Materials," Phys. Rev. Lett. 88, 153901 (2002).

[5] Andrews, D. L. and Hands, I. D., "Second harmonic generation in partially ordered media and at interfaces: Analysis of dynamical and orientational factors," Chem. Phys. 213, 277-294 (1996).

[6] Allcock, P. and Andrews, D. L., "Six-wave mixing: secular resonances in a higher-order mechanism for second-harmonic generation," J. Phys. B: At. Mol. Opt. Phys. 30, 3731-3742 (1997).

[7] Hands, I. D., Lin, S. J., Meech, S. R. and Andrews, D. L., "A quantum electrodynamical treatment of second harmonic generation through phase conjugate six-wave mixing: Polarization analysis," J. Chem. Phys. 109, 10580-10586 (1998).

[8] Lin, S. J., Hands, I. D., Andrews, D. L. and Meech, S. R., "Optically induced second harmonic generation by six-wave mixing: A novel probe of solute orientational dynamics," J. Phys. Chem. A 103, 3830-3836 (1999).

[9] Hands, I. D., Lin, S. J., Mech, S. R. and Andrews, D. L., "Quantum-electrodynamical treatment of second-harmonic generation through phase-conjugate six-wave mixing: Temporal analysis," Phys. Rev. A 62, 023807 (2000).

[10] Dorfman, K. E., Fingerhut, B. P. and Mukamel, S., "Time-resolved broadband Raman spectroscopies: A unified six-wave-mixing representation," J. Chem. Phys. 139, 124113 (2013).

[11] Coles, M. M., Williams, M. D. and Andrews, D. L., "Second harmonic generation in isotropic media: six-wave mixing of optical vortices," Opt. Express 21, 12783-12789 (2013).

[12] Andrews, D. L. and Thirunamachandran, T., "On three-dimensional rotational averages," J. Chem. Phys. 67, 5026-5033 (1977).

[13] Mair, A., Vaziri, A., Weihs, G. and Zeilinger, A., "Entanglement of the orbital angular momentum states of photons," Nature 412, 313-316 (2001).

[14] Franke-Arnold, S., Barnett, S. M., Padgett, M. J. and Allen, L., "Two-photon entanglement of orbital angular momentum states," Phys. Rev. A 65, 033823 (2002).

[15] Romero, J., Giovannini, D., Franke-Arnold, S., Barnett, S. M. and Padgett, M. J., "Increasing the dimension in high-dimensional two-photon orbital angular momentum entanglement," Phys. Rev. A 86, 012334 (2012).

[16] Alison, M. Y., "Angular momentum decomposition of entangled photons with an arbitrary pump," New J. Phys. 13, 053048 (2011).

[17] Franke-Arnold, S., “Orbital angular momentum of photons, atoms, and electrons,” Proc. SPIE 8637, 86370P (2013).

[18] Shwa, D., Shtranvasser, E., Shalibo, Y. and Katz, N., “Controllable motion of optical vortex arrays using electromagnetically induced transparency,” Opt. Express 20, 24835-24842 (2012).

[19] Cao, M. T., Han, L., Liu, R. F., Liu, H., Wei, D., Zhang, P., Zhou, Y., Guo, W. G., Zhang, S. G., Gao, H. and Li, F. L., “Deutsch's algorithm with topological charges of optical vortices via non-degenerate four-wave mixing,” Opt. Express 20, 24263-24271 (2012).

[20] Olivier, N., Débarre, D., Mahou, P. and Beaurepaire, E., “Third-harmonic generation microscopy with Bessel beams: a numerical study,” Opt. Express 20, 24886-24902 (2012).

[21] Franke, S. and Barnett, S. M., “Angular momentum in spontaneous emission,” J. Phys. B: At. Mol. Opt. Phys. 29, 2141 (1996).

[22] Arnaut, H. H. and Barbosa, G. A., “Orbital and intrinsic angular momentum of single photons and entangled pairs of photons generated by parametric down- conversion,” Phys. Rev. Lett. 85, 286-289 (2000).

[23] Franke-Arnold, S., Barnett, S. M., Yao, E., Leach, J., Courtial, J. and Padgett, M., “Uncertainty principle for angular position and angular momentum,” New J. Phys. 6, 103 (2004).

[24] Gibson, G., Courtial, J., Padgett, M., Vasnetsov, M., Pas'ko, V., Barnett, S. and Franke-Arnold, S., “Free-space information transfer using light beams carrying orbital angular momentum,” Opt. Express 12, 5448-5456 (2004).

[25] Berkhout, G. C., Lavery, M. P., Courtial, J., Beijersbergen, M. W. and Padgett, M. J., “Efficient sorting of orbital angular momentum states of light,” Phys. Rev. Lett. 105, 153601 (2010).

[26] Lavery, M. P., Roberston, D., Malik, M., Robenburg, B., Courtial, J., Boyd, R. W. and Padgett, M. J., “The efficient sorting of light's orbital angular momentum for optical communications,” Proc. SPIE 8542, 85421R (2012).

[27] O'Sullivan, M. N., Mirhosseini, M., Malik, M. and Boyd, R. W., “Near-perfect sorting of orbital angular momentum and angular position states of light,” Opt. Express 20, 24444-24449 (2012).

[28] Mirhosseini, M., Malik, M., Shi, Z. and Boyd, R., “Efficient separation of the orbital angular momentum eigenstates of light,” Nat. Commun. 4, 2781 (2013).

* E-mail: david.andrews@physics.org